Biomaterials 31 (2010) 2637–2645

Contents lists available at ScienceDirect

Biomaterials

journal homepage: www.elsevier.com/locate/biomaterials

# Synthesis of a family of amphiphilic glycopolymers *via* controlled ring-opening polymerization of functionalized cyclic carbonates and their application in drug delivery

Fabian Suriano [a], Russell Pratt [c], Jeremy P.K. Tan [b], Nikken Wiradharma [b], Alshakim Nelson [c,*], Yi-Yan Yang [b,*], Philippe Dubois [a,*], James L. Hedrick [c,*]

[a] Center of Innovation and Research in Materials and Polymers (CIRMAP), Laboratory of Polymeric and Composite Materials, University of Mons, 20, Place du Parc, B-7000 Mons, Belgium
[b] Institute of Bioengineering and Nanotechnology, 31 Biopolis Way, Singapore 138669, Singapore
[c] IBM Almaden Research Center, 650 Harry Road, San Jose, CA 95120, USA

ARTICLE INFO

*Article history:*
Received 1 October 2009
Accepted 7 December 2009
Available online 13 January 2010

*Keywords:*
Functional cyclic carbonate
Organocatalytic ring-opening
Amphiphilic polycarbonate
Micelles
Galactose
Drug targeting

ABSTRACT

Polymers bearing pendant carbohydrates have a variety of biomedical applications especially in the area of targeted drug delivery. Here we report the synthesis of a family of amphiphilic block glycopolymers containing D glucose, D galactose and D mannose *via* metal-free organocatalyzed ring-opening polymerization of functional cyclic carbonates generating narrowly dispersed products of controlled molecular weight and end-group fidelity, and their application in drug delivery. These glycopolymers self-assemble into micelles having a high density of sugar molecules in the shell, a size less than 100 nm with narrow size distribution even after drug loading, and little cytotoxicity, which are important for drug delivery. Using galactose-containing micelles as an example, we demonstrate their strong targeting ability towards ASGP-R positive HepG2 liver cancer cells in comparison with ASGP-R negative HEK293 cells although the galactose is attached to the carbonate monomer at 6-position. The enhanced uptake of DOX-loaded galactose-containing micelles by HepG2 cells significantly increases cytotoxicity of DOX as compared to HEK293. This new family of amphiphilic block glycopolymers has great potential as carriers for targeted drug delivery.



## 1. Introduction

Non-cytotoxic and biodegradable polymers which assemble into well-defined nanostructures such as micelles are of increasing interest as a means for drug transport and release. Nanoscale micellar carriers are particularly advantageous for passive drug targeting into solid tumors, as the hyperpermeable angiogenic vasculature of tumor tissues exhibits enhanced permeability and retention of carriers $\leq$100 nm [1]. In contrast to passive drug delivery, active targeting based on specific ligand–receptor interactions has recently received significant attention. Polymers bearing pendant carbohydrates are particularly useful for delivery applications that require the targeting of carbohydrate-binding proteins known as lectins. Protein–carbohydrate interactions mediate a number of biological processes, including cell growth, inflammation, infections and adhesion, *via* multivalent interactions [2–4]. The enhancement in binding, as a consequence of polyvalent interactions, is known as the glycoside cluster effect [5]. Carbohydrate-bearing polymers present a platform for which multiple copies of a saccharide can be presented simultaneously, thus enhancing their affinity and selectivity for lectins. A number of carbohydrate-bearing polymeric architectures have been developed over recent years including dendrimers [6–11], linear polymers [12–15], and micelles [16–18]. The block copolymers bearing the carbohydrates as the targeting groups are expected to have utility in receptor-mediated targeting of genes and drugs to specific tissues/cells [19]. For example, the asialoglycoprotein receptors (ASGP-R) on the surface of hepatocytes have been proposed as a target permitting organ-specific therapy of various diseases [20], including viral [21], parasitic [22], and malignant [21] disorders.

In our effort to create well-defined non-cytotoxic and biodegradable polymeric nanocarriers, carbohydrate-bearing block copolymers have been synthesized *via* organocatalytic ring-opening polymerization (ROP) of functional trimethylene

* Corresponding authors.
*E-mail addresses:* alshak@us.ibm.com (A. Nelson), yyyang@ibn.a-star.edu.sg (P. Yang), philippe.dubois@umh.ac.be (P. Dubois), hedrick@almaden.ibm.com (J.L. Hedrick).

0142-9612/$ – see front matter © 2009 Elsevier Ltd. All rights reserved.
doi:10.1016/j.biomaterials.2009.12.022

carbonate (TMC) derivatives. Herein, we describe the synthesis and polymerization of cyclic carbonates containing diacetonide-protected glucose, galactose and mannose to afford carbohydrate-bearing polymers, and demonstrate that these sugar-functionalized polycarbonate block copolymers can self-assemble into micelles having surfaces with a high density of sugar molecules. Glucose-, galactose and mannose-coated micelles are designed for targeting cancer (as many types of cancer cells over-express glucose transporters) [23], liver [24–26] and dendritic [27] cells, respectively. We will use galactose-containing micelles as an example, and prove their ability of loading doxorubicin (a drug used for liver cancer treatment) as well as targeting liver cancer cells through qualitative and quantitative cellular uptake, competition and cytotoxicity studies.

## 2. Materials and methods

### 2.1. Materials

Reagents were commercially available from Aldrich and used without any other purification unless otherwise noted. 5-Methyl-5-carboxyl-1,3-dioxan-2-one (MCDO) was synthesized as previously reported [28]. TU was prepared as previously reported [29] and dried by stirring in dry THF over $CaH_2$, filtering, and removing solvent under vacuum. 1,8-Diazabicyclo[5.4.0]undec-7-ene (DBU; 98%) and benzyl alcohol were stirred over $CaH_2$, vacuum distilled, then stored over molecular sieves (3 Å). Melting points of monomers were recorded with a capillary tube melting point apparatus and were uncorrected. Doxorubincin hydrochloride (DOX), pyrene, triethylamine (TEA), N, N-dimethylacetamide (DMAc), dimethyl sulfoxide (DMSO), 3-(4, 5-dimethylthiazolyl-2)-2, 5-diphenyl tetrazolium bromide (MTT) and asialofetuin (ASF) were purchased from Sigma, U.S.A. and used as received. HepG2 liver carcinoma and HEK293 human embryonic kidney cell lines were obtained from ATCC, U.S.A. and cultured according to ATCC's recommendation.

### 2.2. Polymer synthesis

#### 2.2.1. Synthesis of 1,2;5,6-Di-O-isopropylidene-3-O-MCDO-D-glucofuranose (IGFC) (**3c**)

MCDO (2.0 g; 12.5 mmol) was dissolved in dry THF (30 ml) with 3 drops of DMF. A solution of oxalyl chloride (1.75 g; 13.8 mmol) in dry THF (12 ml) was added and the mixture was allowed to react one more hour under stirring and nitrogen flow. Volatiles were then removed under vacuum and $^1$H NMR analysis evidenced a complete conversion of the acyl chloride. This last was redissolved in THF (30 ml) and a solution of 1,2;5,6-Di-O-isopropylidene-D-glucofuranose (3.0 g; 11.5 mmol) and dried triethylamine (1.51 g; 15 mmol) in THF was added, causing the formation of a white precipitate. The mixture was stirred at 40 °C during 48 h before filtration of the triethylamine salt and concentration of the crude product under reduced pressure. Purification was realized by recrystallization in diethyl ether to give a white solid, mp 132–134 °C. Yield = 1.62 g (50%). $^1$H NMR: $\delta$ 5.92 (d, $J$ = 3.6 Hz, 1H, H-a), 5.40 (d, $J$ = 2.9 Hz, 1H, H-c), 4.71 (m, 2H, H-j), 4.47 (d, $J$ = 3.6 Hz, 1H, H-b), 4.26–4.12 (m, 5H, H-d + H-e + H-f + H-j'), 4.01 (m, 1H, H-g), 1.54–1.32 (5 s, 15H, H-h + H-i). $^{13}$C NMR: $\delta$ 181.5, 171.2, 147.1, 113.1, 110.0, 105.4, 83.6, 80.5, 73.4, 73.2, 72.8, 68.3, 27.1, 27.0, 26.6, 25.5, 17.8.

#### 2.2.2. Synthesis of 2,3;5,6-Di-O-isopropylidene-3-O-MCDO-D-mannofuranose (IMFC) (**3b**)

This compound was synthesized according to the same procedure used for IGFC, using 2,3; 5,6-Di-O-isopropylidene-D-mannofuranose as the coupling alcohol (3.0 g; 11.5 mmol) and purified by recrystallization in diethyl ether to give a yellowish solid, mp 142–144 °C. Yield = 2.55 g (55%). $^1$H NMR: $\delta$ 6.22 (s, 1H, H-a), 4.89 (dd, $J_1$ = 5.8 Hz, $J_2$ = 3.5 Hz, 1H, H-b), 4.72 (d, $J$ = 5.8 Hz, 2H, H-d), 4.66 (m, 2H, H-j), 4.41 (m, 1H, H-c), 4.22 (m, 2H, H-j'), 4.11 (dd, $J_1$ = 8.8 Hz, $J_2$ = 2.4 Hz, 2H, H-e), 4.03 (m, 2H, H-f + H-g), 1.50–1.33 (5 s, 15H, H-h + H-i). $^{13}$C NMR: $\delta$ 170.1, 147.2, 114.0, 109.9, 103.0, 85.3, 83.5, 79.5, 73.3, 73.1, 67.2, 40.8, 27.3, 26.3, 25.5, 25.0, 17.6.

#### 2.2.3. Synthesis of 1,2;3,4-Di-O-isopropylidene-3-O-MCDO-D-galactopyranose (IGPC) (**3a**)

This compound was synthesized according to the same procedure used for IGFC, using 1,2;3,4-Di-O-isopropylidene-D-galactopyranose as the coupling alcohol (3.0 g; 11.5 mmol) and purified by column chromatography (silica, 2:1 ethyl acetate/hexanes) leading to the desired product as an oil slowly crystallizing in a white solid, mp 117–120 °C. Yield = 2.36 g (51%). $^1$H NMR: $\delta$ 5.54 (d, $J$ = 5.3 Hz, 1H, H-a), 4.73 (m, 2H, H-h), 4.64 (dd, $J_1$ = 8.0 Hz, $J_2$ = 2.7 Hz, 1H, H-c), 4.44 (dd, $J_1$ = 11.7 Hz, $J_2$ = 3.9 Hz, 1H, H-b), 4.35 (m, 2H, H-f + H-f'), 4.22 (m, 3H, H-h' + H-d), 4.04 (ddd, $J_1$ = 8.8 Hz, $J_2$ = 3.9 Hz, 1H, H-e), 1.51–1.35 (5 s, 15H, H-g + H-i). $^{13}$C NMR: $\delta$ 173.3, 147.2, 110.2, 109.2, 96.6, 73.3, 71.2, 71.1, 70.8, 66.2, 65.2, 40.5, 26.3, 25.3, 24.8, 18.2.

#### 2.2.4. General procedure for block copolymerization

TMC (100 mg, 1 mmol), TU (17.5 mg, 0.05 mmol) and DBU (7.5 mg, 0.05 mmol) were mixed together in a vial. 0.5 ml of a solution of benzyl alcohol (0.04 M) in dichloromethane was added and the mixture was stirred at room temperature during 3 h. An aliquot was taken and quenched with benzoic acid, dried and redissolved in $CDCl_3$ for the first block conversion calculation. **3a** (200 mg, 0.5 mmol) (Fig. 1A and B) was added to the polymer mixture for chain extension during 90 min. An aliquot was again taken for conversion data and the remaining solution was quenched with benzoic acid, precipitated in methanol, filtered and dried overnight at 40 °C.

#### 2.2.5. General procedure for isopropylidene selective hydrolysis

The protected polymer (0.25 g) was dissolved in 2.5 ml of a 4:1 formic acid aqueous solution during 48 h. Dialysis against water using 3.5 kDa cutoff membrane was performed during 48 h changing water every 6 h. The micellar solution was then transferred in a vial and freeze-dried to give a white powder in good yields (90%). NMR spectra were recorded in DMSO-$d_6$.

### 2.3. Molecular weight determination

Molecular weight ($M_w$) of the polymers were determined by gel permeation chromatography (GPC) performed in THF at 30 °C using a Waters chromatograph equipped with four 5 μm Waters columns (300 mm × 7.7 mm) connected in series with increasing pore size (10, 100, 1000, $10^5$, $10^6$ Å), a Waters differential refractometer for refractive index (RI) detection and a 966 photodiode array detector, and calibrated with polystyrene standards (750 − (2 × $10^6$) g mol$^{-1}$).

### 2.4. Nuclear magnetic resonance (NMR)

$^1$H and $^{13}$C NMR spectra were obtained on a Bruker Avance 400 instrument operated at 400 MHz, using $CDCl_3$ solutions unless otherwise noted. In order to study the core/shell structure of the micelles, $^1$H NMR spectra of the micelles were measured in $D_2O$.

### 2.5. Fluorescence measurements

The critical micelle concentrations (CMC) of the polymers in de-ionized (DI) water or phosphate-buffered saline (PBS, pH 7.4) were determined by fluorescence spectroscopy using pyrene as the probe. The fluorescence spectra were recorded by an LS 50B luminescence spectrometer (Perkin Elmer, U.S.A.) at 25 °C. The polymer samples were equilibrated for 10 min before any measurements were made. Aliquots of pyrene in acetone solution (6.16 × $10^{-5}$ M, 10 μL) were added to containers, which were left in air to evaporate acetone. Polymer solutions (1 mL) at varying concentrations were added into the pyrene containers and left to equilibrate for 24 h. The final pyrene concentration in each sample is 6.16 × $10^{-7}$ M. The emission spectra were scanned from 360 to 410 nm at an excitation wavelength of 339 nm while the excitation spectra were scanned from 300 to 360 nm at an emission wavelength of 395 nm. Both the excitation and emission bandwidths were set at 2.5 nm. The intensity (peak height) ratio of $I_{337}/I_{334}$ from the excitation spectra was analyzed as a function of polymer concentration (Fig. S1). The CMC was taken from the intersection between the tangent to the curve at the inflection and tangent of the points at low concentrations.

### 2.6. Micelles preparation

Blank micelles were prepared by dissolving the polymers in water directly and stirred overnight. For the DOX-loaded micelles, they were prepared by a combination of sonication and membrane dialysis method. In brief, the polymer (10 mg) was dissolved in 0.5 mL of DMAc. DOX (7 mg) was neutralized with 3 mol excess of TEA in 1.5 mL DMAc. This neutralized DOX solution was added into the polymeric solution and vortexed for 5 min. The drug and polymer solution was added dropwise to DI water (10 mL) and sonicated for 10 min. After which, the mixture was dialyzed against DI water using a 1000 Da molecular weight cutoff membrane (Spectra/Por 7, Spectrum Laboratories Inc.) for 48 h. The particles were collected by lyophilization for 2 days. The amount of DOX-loaded was measured by dissolving a known amount of DOX-loaded micelles in 1 mL of DMSO and measuring the absorbance using a UV–vis spectrophotometer (UV 2501PC Shimadzu, Japan) at 480 nm. DOX loading level was calculated based on the following formula:

$$\text{Actual loading level (wt\%)} = \frac{\text{mass of DOX extracted from polymer}}{\text{mass of DOX loaded polymer initially used}} \times 100\%$$

### 2.7. Laser light scattering measurements

Dynamic light scattering (DLS) experiments of the freshly prepared micelles were performed on a Brookhaven BI-200SM goniometer system (Brookhaven, USA) to determine the particle size. Briefly, polymer solution with a concentration of 0.5 mg/mL was prepared and filtered using 0.45 μm PVDF filter before measurement

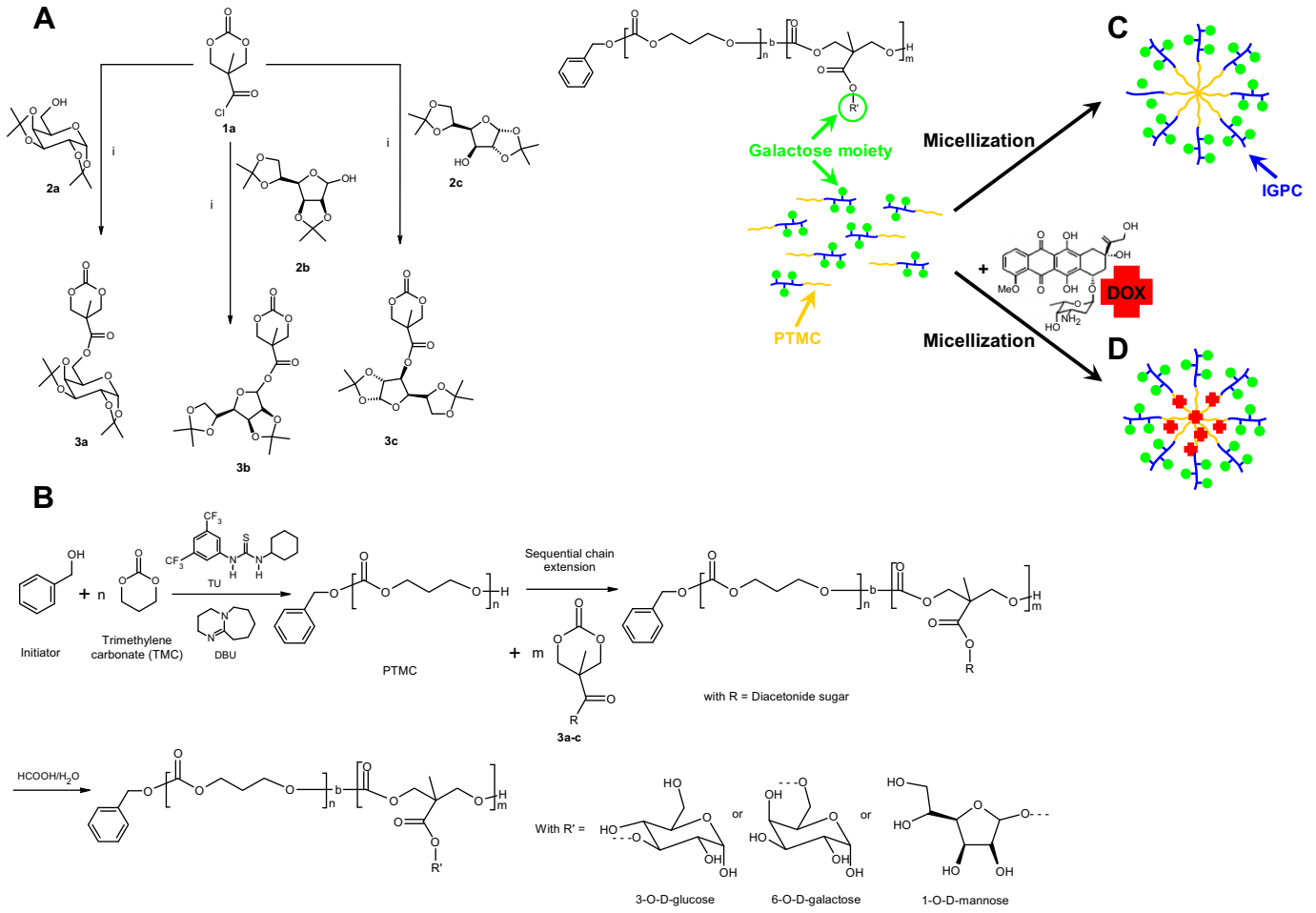


**Fig. 1.** Synthesis of sugar-bearing cyclic carbonate monomers (A) (conditions: (i) $NEt_3$, THF, 40 °C, 24 h, 50–55%), amphiphilic block glycopolymers by sequential polymerization followed by selective deprotection (B), schematic presentation of self-assembly of block glycopolymers into micelles (C) and drug loading (D). 3a: IGPC; 3b: IMFC; 3c: IGFC.

was conducted. After the measurement, non-negative least-squares (NNLS) were used to fit the distribution curve and the fitting obtained was found to be with a $R^2$ value of at least 0.98. The light source is a power adjustable vertically polarized 75 mW HeNe ion laser with a wavelength of 633 nm. The measurement was conducted at 25 °C with a scattering angle of 90°. The particle size measurement was repeated for 5 runs and the data were reported as the average mean diameter for 5 runs.

### 2.8. Transmission electron microscopy (TEM)

The morphologies of the micelles were observed under a FEI Tecnai $G^2$ F20 electron microscope using an acceleration voltage of 200 keV. To prepare the TEM samples, several drops of the micelles solution containing 0.2% (w/v) of phosphotungstic acid, which were incubated for 30 min, were placed on a formvar/carbon coated 200 mesh copper grid and left to dry under room temperature.

### 2.9. Stability of sugar-containing micelles in serum-containing PBS

Stability of the sugar-containing micelles in PBS containing 10% (v/v) fetal bovine serum (FBS) was studied at 37 °C by particle size change as a function of time. Size measurements were taken at 5 min, 15 min, 30 min, 1 h, 2 h, 4 h, 6 h, and 8 h.

### 2.10. In vitro drug release

DOX-loaded micelles solutions at a concentration of 1 mg/mL (5 mL) were transferred to dialysis membrane tubes with a molecular weight cutoff of 1000 Da. The tubes were then immersed in a beaker containing 50 mL PBS, which was shaken at a speed of 100 rev/min, at 37 °C. At specific time intervals, 1 mL of the release medium was withdrawn and replaced with fresh PBS. The DOX content in the samples were analyzed using the UV–vis spectrophotometer at 480 nm.

### 2.11. Cellular uptake-qualitative analysis through confocal laser scanning microscopy (CLSM)

The cellular uptake of DOX when delivered using free DOX formulation, galactose-containing micelles or glucose-containing micelles was studied qualitatively in HepG2 and HEK293 cells using a confocal laser scanning microscope. HepG2 cells carrying over-expression of asialoglycoprotein receptor (ASGP-R+) were used for the experimental group for galactose-coated micelles, while HEK293 cells, bearing no over-expression of ASGP-R (ASGP-R -) were used as a control group. The cells were first seeded onto a 4 well-cover slip borosilicate glass chamber (NUNC) at a seeding density of 40,000 cells/well and grown overnight in Dulbecco's modified Eagle's medium (DMEM) supplemented with 10% FBS, 2 mM L-glutamine, 50 units/mL penicillin and 50 μg/mL streptomycin. On the following day, the cells were treated with free DOX (1 mg/L), DOX-loaded galactose-containing micelles (1 mg/L equivalent DOX concentration), and DOX-loaded glucose-containing micelles (1 mg/L equivalent DOX concentration) for 3 h. The cells were then washed thoroughly with PBS for 5 times. Both free DOX and DOX-loaded glucose-containing micelles were served as the controls towards ASGP-R mediated endocytosis uptake mechanism. The measurements were done with excitation and emission wavelengths of 532 nm and 595 nm respectively.

### 2.12. Cellular uptake-quantitative analysis through flow cytometry

The cellular uptake of DOX was further studied quantitatively in HepG2 and HEK293 cells *via* flow cytometry using the free DOX, glucose-containing micelles, galactose-containing micelles formulations. The cells were seeded onto 12-well plate at a seeding density of 1,000,000 cells per well, and further grown for 24 h. Following this, the cells were treated with free DOX (1 mg/L), DOX-loaded galactose-containing micelles (1 mg/L equivalent DOX concentration), and DOX-loaded glucose-containing micelles (1 mg/L equivalent DOX concentration) for 3 h. After the incubation period, the cells were washed thoroughly with PBS, trypsinized, and harvested by centrifugation (1500 rpm, 10 min). The cell pellet was then

resuspended in PBS and measured for the fluorescent intensity per cell. The fluorescent intensity measurement was referenced to that given by HepG2 or HEK293 cells without any drug treatments to eliminate the possibility of auto-fluorescent phenomenon produced by the cells. The measurements were done with excitation and emission wavelengths of 532 nm and 595 nm respectively.

### 2.13. Competition assay

ASF as an inhibitor was added to the HepG2 cells at various concentrations (0, 0.5, 1.0 and 4.0 mg/mL) and incubated for an hour. The cells were then washed with PBS before being treated with the DOX-loaded galactose-containing micelles at an equivalent DOX concentration of 1 mg/L for 3 h. After the incubation, the cells were washed thoroughly, trypsinized, and harvested by centrifugation. The cell pellet was resuspended in PBS and measured for fluorescent intensity per cell. The fluorescent intensity measurement was referenced to that given by HepG2 cells without any drug treatments to eliminate the possibility of auto-fluorescent phenomenon produced by the cells. The measurements were done with excitation and emission wavelengths of 532 nm and 595 nm respectively.

### 2.14. Cytotoxicity test

The cytotoxicity of free DOX, sugar-containing micelles and DOX-loaded sugar-containing micelles were examined *via* MTT assay. HepG2 and HEK293 cells were seeded in a 96-well plate at a density of 8000 cells per well in 100 μL of DMEM supplemented with 10% FBS, 2 mm L-glutamine and 1% penicillin-streptomycin, and incubated for 24 h at 37 °C in 5% $CO_2$. The free DOX, sugar-containing micelles and DOX-loaded sugar-containing micelles solutions were filtered with a 0.22 μm syringe filter and diluted with DMEM to achieve different concentrations. 100 μL of the pre-prepared sample solution was used to replace the medium in each well, and the plates were returned to the incubator and maintained in 5% $CO_2$, at 37 °C, for 48 h. Fresh growth media and 20 μL aliquots of MTT stock solution (5 mg/mL in PBS) totaling 120 μL were used to replace the media and incubated for 4 h. The media were completely removed and 150 μL of DMSO was added into each well to dissolve the formazane crystals formed by viable cells. Each sample was tested in eight replicates per plate and assayed at 550 and 690 nm using a microplate reader (PowerWave X, Bio-Tek Instruments). The absorbance readings of the formazan crystals were taken to be that at 550 nm subtracted by that 690 nm. The results were expressed as a percentage of the absorbance of the blank control.

## 3. Results and discussion

### 3.1. Synthesis of sugar-functionalized poly(carbonate) block copolymers

Sugar-substituted cyclic carbonates were synthesized based on the acyl chloride form of an acid functional carbonate scaffold, **1a** [28], derived from bis(hydroxymethyl) propionic acid, a common building block for non-cytotoxic dendrimers [30,31]. **1a** was then reacted with **2a**, **2b** or **2c** in the presence of triethylamine to give sugar-bearing carbonate monomers **3a**–**3c**, respectively (Fig. 1A). The crude products were filtered off, extracted and purified by either recrystallization or column chromatography.

The ROP of the sugar-based monomers was then performed using the superbasic amidine 1,8-diazabicyclo[5,4,0]undec-7-ene (DBU) catalyst with a thiourea TU co-catalyst, initiated from benzyl alcohol. High conversion of monomer into polymer was achieved within 3 h at room temperature (Table 1). The molecular weights were determined by $^1$H NMR spectroscopy, comparing the anomeric proton signal of the repeating units (5.50 ppm for IGPC, 5.87 ppm for IGFC and 6.15 ppm for IMFC) with the methylene protons of the initiating benzyl alcohol (5.19 ppm), which showed good correlation with targeted molecular weights. Moreover, narrow polydispersities and monomodal molecular weight distributions were obtained. These combined data demonstrated the efficacy of polymerization using organocatalytic ROP yielding narrowly dispersed polymers of predictable molecular weights. Although a number of cyclic carbonate monomers have been synthesized and polymerized in the past by more conventional anionic and organometallic ROP methods [32], excessively bulky substituents (e.g. 2,2-diphenyl) proved to render ring-opening of the carbonate thermodynamically unfavorable [33–36]. Interestingly, for monomers **3a**–**c**, substitution at the 5-position of the carbonate ring does not seem to interfere sterically with the polymerization reaction.

**Table 1**
Homopolymerization of carbohydrate-based monomers.

| Monomer | Conv.[a] (%) | Time (hours) | Targeted $M_n$ (g.mol$^{-1}$) | Reached $M_n$[a] (g.mol$^{-1}$) | PDI[b] |
|---|---|---|---|---|---|
| 3a | 93 | 3 | 20,200 | 17,000 | 1.20 |
| 3b | 93 | 3 | 20,200 | 17,800 | 1.27 |
| 3c | 86 | 3 | 20,200 | 19,000 | 1.28 |

Conditions: 1 M in monomer, 0.02 M in BzOH, 0.05 M in DBU, 0.05 M in TU, $CH_2Cl_2$, R.T.
[a] As obtained by $^1$H NMR.
[b] As obtained by GPC *vs.* polystyrene standards.

Block copolymers were prepared in a one-pot, two-step process using a sequential polymerization approach. The PTMC block was first synthesized to near quantitative conversion (98%, $M_n = 5000$ g/mol, PDI = 1.1), followed by the addition of a second monomer (**3a**, **3b or 3c**) to the reaction mixture for the growth of the second block (Fig. 1B). The synthesis and chain extension of the copolymers was monitored by $^1$H NMR and GPC. The GPC chromatograms show the expected increase in molecular weight after the addition of the second monomer, as evidenced by a shift of the polymer trace to shorter elution time (Fig. S2). The results of block copolymer formation with three different lengths of the sugar-functionalized block were summarized in Table 2, demonstrating that exceptional control was achieved for each of the block glycocopolymers.

The acetonide protecting groups along the glycopolymer chains were selectively removed with aqueous formic acid solution to regenerate hydroxyl groups. $^1$H NMR showed an upfield shift of the saccharide peaks in addition to the disappearance of the isopropylidene groups, while SEC exhibited narrow monomodal distributions, confirming the selective hydrolysis of the acetonide protecting groups.

### 3.2. Formation of micelles: critical micellization concentration (CMC)

The sugar-functionalized polycarbonate block copolymers can self-assemble into micelles in aqueous solution (Fig. 1C), which is evidenced by the existence of their low critical micellization concentrations (CMC). The CMC values of the glucose- and galactose-functionalized block copolymers with molecular weights of 13,200 and 14,200 respectively, were measured using a fluorescence technique. Pyrene was chosen as the fluorescent probe as it can be portioned into the hydrophobic domains of the micelles, resulting in a change in its photophysical properties. In the

**Table 2**
Block copolymerization of 3-type sugar carbonates with various compositions.

| Monomer | Conv. sugar monomer[a] (%) | Targeted $M_n$ (g.mol$^{-1}$) | Reached $M_n$[a] (g.mol$^{-1}$) | PDI[b] |
|---|---|---|---|---|
| 3a | 88 | 10,400 | 9300 | 1.24 |
| 3a | 92 | 15,300 | 14,200 | 1.26 |
| 3a | 93 | 25,300 | 25,000 | 1.25 |
| 3b | 87 | 10,400 | 8400 | 1.25 |
| 3b | 90 | 15,300 | 12,700 | 1.25 |
| 3b | 91 | 25,300 | 26,200 | 1.26 |
| 3c | 75 | 10,400 | 9100 | 1.22 |
| 3c | 94 | 15,300 | 13,200 | 1.23 |
| 3c | 94 | 25,300 | 22,900 | 1.25 |

Conditions: PTMC block formation, 1 M in TMC, 0.02 M BzOH, 0.05 M DBU, 0.05 M TU, $CH_2Cl_2$, R.T., 3 h. Chain extension, 0.25–1 M in monomer 3a–c, 0.05 M DBU, 0.05 M TU, $CH_2Cl_2$, R.T., 90 min.
[a] As obtained by $^1$H NMR.
[b] As obtained by GPC *vs.* polystyrene standards. a: galactose; b: mannose; c: glucose.

excitation spectra of pyrene in the presence of the block copolymers, fluorescence intensity increased with increasing polymer concentration, while a gradual red shift of the third peak from 334 to 337 nm could be monitored (data not shown), indicating the change in vibration structure of pyrene emission. From the work reported by Wilhelm et al. the intensity ratio of $I_{337}/I_{334}$ is dependent on polymer concentration [37]. At lower polymer concentrations, the intensity ratio changed slightly, however, it increased significantly with the transfer of pyrene from a polar to more hydrophobic domain, i.e. after micelle formation. The CMC values of the glucose- and galactose-functionalized poly(carbonate) block copolymers in DI water were 7.1 and 5.0 μg/mL, respectively (Fig. S1) (Table 3), which were also measured in a simulated physiological solution, i.e. PBS (pH 7.4), being 5.6 and 3.5 μg/mL respectively, slightly lower than those determined in water due to the presence of salts in PBS. The low CMC values indicate that the micelles can be formed at low concentrations, allowing the use in very dilute medium such as body fluids (dilution effect after *i.v.* injection).

TEM clearly shows the formation of spherical galactose-containing micelles (Fig. 2(a)). These micelles have an average size of 35 nm and narrow size distribution (PDI = 0.09), ideal for long circulation times.

### 3.3. Core/shell structure

The core/shell structure of the micelles was demonstrated by $^1$H NMR spectroscopy of the sugar-containing micelles dissolved in $D_2O$. The peaks between 3.5 and 4.5 ppm can be assigned to the galactose ring protons and the sharp peak at 5.25 ppm corresponses to the anomeric peak of α-D-galactose moieties. Moreover, the peak at 1.2 ppm is the signal corresponding to the methyl of the polycarbonate backbone bearing the sugar. Moreover, there is no clear evidence of the PTMC backbone peaks, consistent with a collapsed hydrophobic core and a core/shell morphology. These combined data indicate that diblock copolymers tend to self-assemble into micelles with a core/shell structure having a sugar-bearing shell and a PTMC core.

### 3.4. Particle size of blank and DOX-loaded sugar-containing micelles

The size and size distribution of the blank sugar-containing micelles and DOX-loaded sugar-containing micelles in DI water and PBS (pH 7.4) are listed in Table 3. The size and size distribution were not affected significantly when measured in PBS. The polydispersity (PDI) values obtained from dynamic light scattering (DLS) measurements indicate that the micelles have a narrow size distribution. Therefore, they may yield a more desirable biodistribution and constant drug release profile as compared to micelles formed from conventional block copolymers with wide size distribution. Average diameter of the blank and DOX-loaded sugar-containing micelles was less than 100 nm, thus making them less susceptible to clearance by the reticuloendothelial system (RES). An increase in diameter after loading with DOX was due to the enlargement of the hydrophobic core. After the incorporation of DOX, the morphology of the micelles was not altered as shown in Fig. 2(b). Furthermore, as listed in Table 3, the aggregation numbers and hydrodynamic diameters of the glucose- and galactose-containing block copolymers are consistent with the formation of spherical micelles, which typically contains 16–60 unimers per micelle and with a hydrodynamic diameter of 20–60 nm [38]. From the aggregation number (18) of galactose-functionalized polymer and number (38) of galactose molecules in each polymer molecule, the number of galactose molecules in the shell of the micelle was estimated to be 684.

**Table 3**
Properties of sugar-functionalized block copolymers and their blank micelles as well as DOX-loaded micelles.

| Samples | CMC (mg/mL) | Diameter (nm) | PDI[a] | $N_g$ |
|---|---|---|---|---|
| Glucose-functionalized polymer | 7.1 (5.6) | 36 ± 5 (29 ± 2) | 0.1 ± 0.01 (0.1 ± 0.02) | 20 (18) |
| Galactose-functionalized polymer | 5.0 (3.5) | 35 ± 4 (29 ± 5) | 0.09 ± 0.01 (0.11 ± 0.02) | 19 (18) |
| DOX-loaded glucose-containing micelles | | 65 ± 6 | 0.12 ± 0.03 | |
| DOX-loaded galactose-containing micelles | | 70 ± 7 | 0.15 ± 0.03 | |

[a] Size and polydispersity values obtained from DLS measurements in which lower values indicate more narrowly dispersed micelles. The values in parenthesis are measured in PBS (pH 7.4).

### 3.5. In vitro stability of the sugar-coated micelles

The stability of both the glucose- and galactose-containing micelles was studied in PBS containing 10% FBS at 37 °C by monitoring particle size change as a function of time. The stability of the sugar-coated micelles is demonstrated by the absence of large aggregates and the maintenance of particle size. As seen in Fig. S3, the size of the micelles remained unchanged for 8 h, indicating that the presence of serum proteins did not affect the stability of the micelles due to the hydrophilic nature of the sugar on the surface of the micelles.

### 3.6. DOX loading level and in vitro drug release

Doxorubicin was loaded into sugar-containing micelles *via* a membrane dialysis method (Fig. 1D) with varying the initial amount of DOX added. The highest loading level of DOX achieved was 9.3% at an initial DOX amount of 7 mg (Fig. 3).

*In vitro* DOX release from the DOX-loaded micelles was studied in PBS (pH 7.4) at 37 °C (Fig. 4). DOX release was sustained over 10 h, and DOX release from the glucose- and galactose-containing micelles shared a similar release profile.

### 3.7. Cellular uptake of DOX

To evaluate the possibility of using galactose-containing micelles for drug targeting to liver cells, we studied uptake of DOX by HepG2 cells with over-expression of ASGP-R and HEK293 cells without expression of ASGP-R using galactose-containing micelles or glucose-containing micelles. ASGP-R can bind galactose residues strongly, inducing ASGP-R mediated endocytosis of galactose-containing micelles [39]. DOX molecules could emit fluorescent signals at 595 nm when excited at 532 nm. This allows the study of cellular uptake of the free DOX or DOX-loaded sugar-containing micelles through confocal microscopy or flow cytometry. Fig. 5(a–f) shows confocal images of HepG2 (a-c) and HEK293 (d-f) cells after incubation with free DOX and DOX-loaded glucose- or galactose-containing micelles at the same concentration of DOX (1 mg/L) for 3 h. Red colour regions indicate DOX molecules. The cellular uptake of free DOX is based on a passive diffusion pathway, whereas glucose-containing micelles were taken up by HepG2 and HEK293 cells *via* non-specific endocytosis and/or *via* glucose transporters [23]. Fig. 5(a–c) clearly shows that ASGP-R mediated endocytosis led to greater uptake of DOX by HepG2 cells when compared to the free diffusion pathway and non-specific endocytosis/glucose transporters route. However, when the DOX-loaded galactose-containing micelles were incubated with HEK293 cells, there is not

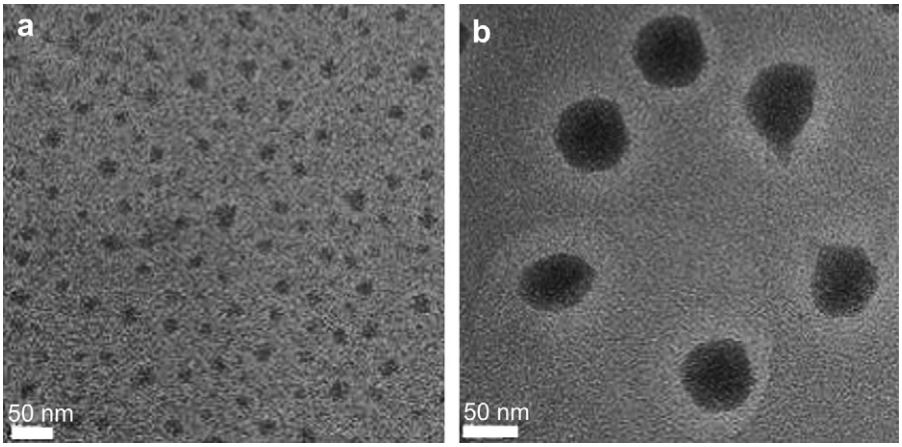


**Fig. 2.** TEM images of (a) galactose-containing micelles and (b) DOX-loaded galactose-containing micelles in DI water.

much difference in the red intensity as compared to the DOX-loaded glucose-containing micelles (Fig. 5(d–e)). Importantly, the red intensity in HepG2 cells was much higher than that in HEK293 cells when galactose-conatining micelles were used, demonstrating targeting ability of galactose-containing micelles towards HepG2 cells.

The cellular uptake of DOX was further analyzed quantitatively *via* flow cytometry. As shown in Fig. 6, the cellular uptake of DOX was much higher (2–3 fold increase) in ASGP-R positive HepG2 cells when delivered by the galactose-containing micelles as compared to the free DOX formulation and the glucose-containing micelles. However, the cellular uptake of DOX in ASGP-R negative HEK293 cells was similar for all three formulations. For the free DOX formulation and glucose-containing micelles, there was no significant difference in the uptake of DOX by HepG2 and HEK293 cells. However, the uptake of DOX by HepG2 cells was more than 2 times higher than that by HEK293 cells when delivered by the galactose-containing micelles. These findings further demonstrate the targeting ability of the galactose-containing micelles towards HepG2 cells.

### 3.8. Competition assay

Uptake mechanism of DOX-loaded galactose-containing micelles by HepG2 cells was studied by a competition assay. Asialofetuin (ASF) is a natural ligand for the ASGP-R. Therefore, ASF molecules should compete with the galactose-containing micelles for binding of ASGP-R provided the ASGP-R mediated endocytosis is a major mechanism of cellular uptake in HepG2 cells [40,41]. As shown in Fig. 7, the cellular uptake of DOX decreased with increasing ASF concentration, indicating that ASF inhibited the cellular uptake of the galactose-cntaining micelles, and the uptake of the galactose-containing micelles in HepG2 cells was through ASGP-R mediated endocytosis.

### 3.9. Cytotoxicity of sugar-containing micelles, free DOX and DOX-loaded sugar-containing micelles

The cytotoxicity of DOX was tested against ASGP-R positive HepG2 and ASGP-R negative HEK293 cells using the galactose-containing micelles in comparison with the free DOX formulation and glucose-containing micelles. It is important to note that both glucose- and galactose-functionalized polymers did not have significant cytotoxicity against HepG2 and HEK293 cells at concentrations up to 300 μg/mL (Fig. S4). As shown in Fig. 8a, at the same concentration, DOX suppressed the proliferation of HepG2 cells much more efficiently when delivered by the galactose-containing micelles than free DOX and glucose-containing micelle formulations, and the $IC_{50}$, a concentration of DOX at which 50% of the cells are killed, for free DOX, DOX-loaded

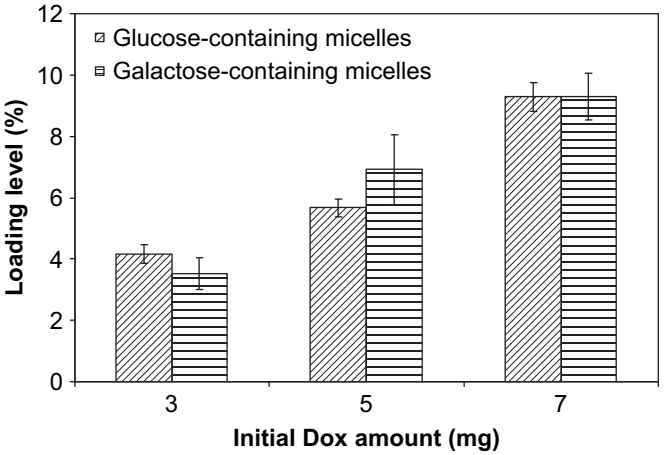


**Fig. 3.** Effect of initial DOX content on the final loading level of sugar-containing micelles.

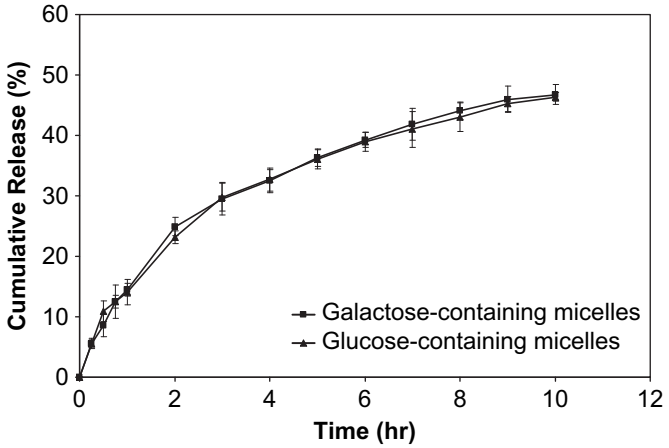


**Fig. 4.** *In vitro* release profiles of DOX-loaded sugar-containing micelles in PBS (pH 7.4) at 37 °C.

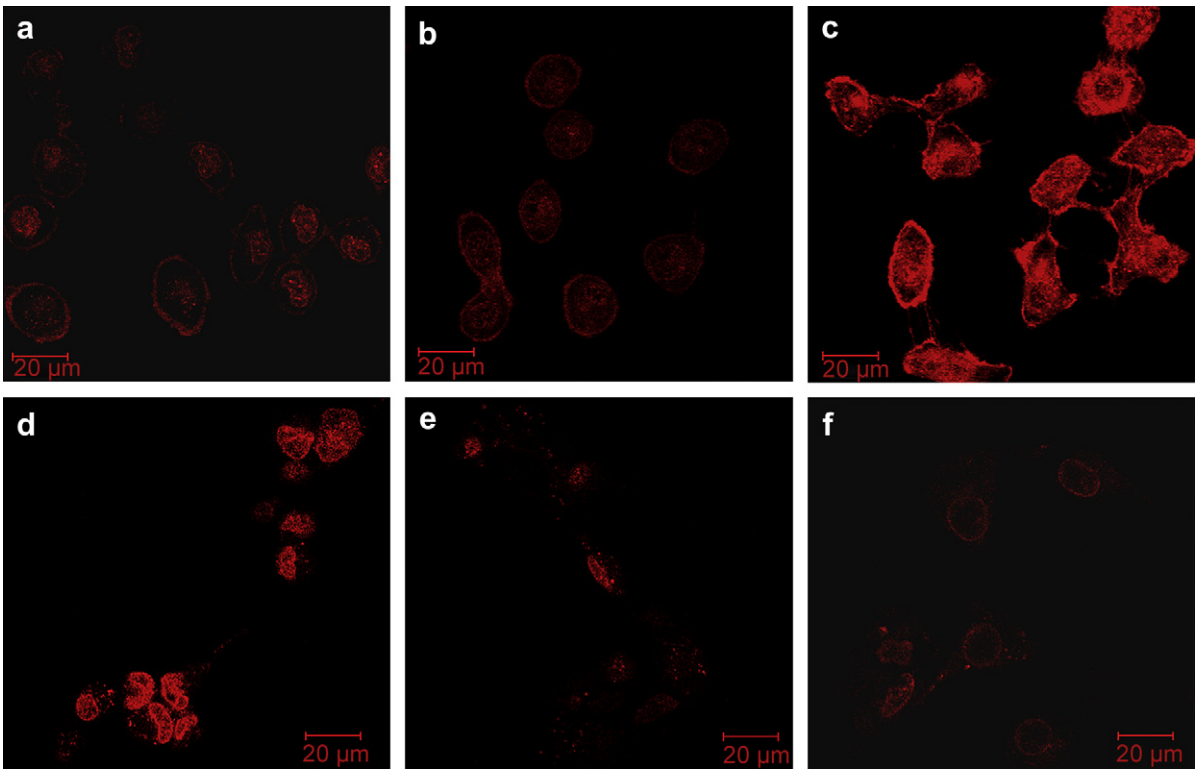


**Fig. 5.** Cellular uptake of galactose-containing micelles. Confocal images of HepG2 (a–c) and HEK293 (d–f) cells after incubated with (a, d) free DOX, (b, e) DOX-loaded glucose-containing micelles and (c, f) DOX-loaded galactose-containing micelles for 3 h at a DOX concentration of 1 mg/L. Size of the scale bars: 20 μm.

glucose- and galactose-containing micelles was estimated to be 0.45, 0.75 and 0.20 μg/mL respectively. The improved cytotoxicity of DOX achieved with the galactose-containing micelles was due to greater cellular uptake of DOX (Figs. 5 and 6). However, in HEK293 cells (Fig. 8b), the cytotoxicity of DOX was similar when delivered by the glucose-containing micelles and the galactose-containing micelles because the cellular uptake of DOX was similar in HEK293 cells when delivered by these two formulations (Figs. 5 and 6). For example, the $IC_{50}$ for free DOX, DOX-loaded glucose- and galactose-containing micelles was 0.30, 0.51 and 0.49 μg/mL respectively. These findings indicate that the galactose-containing micelles not only provided targeting ability towards ASGP-R positive HepG2 cells but also increased cytotoxicity of the enclosed DOX against the cells. Moreover, while most galactose-bearing glycoconjugates are appended to the polymer backbone at the 1-position of the pyranose ring [11], our results demonstrate that ASGP-R recognizes galactopyranosides appended at the 6-position. Further investigations are underway to compare the affinity and selectivity of ASGP-R for 1- versus 6- substituted galactosides.

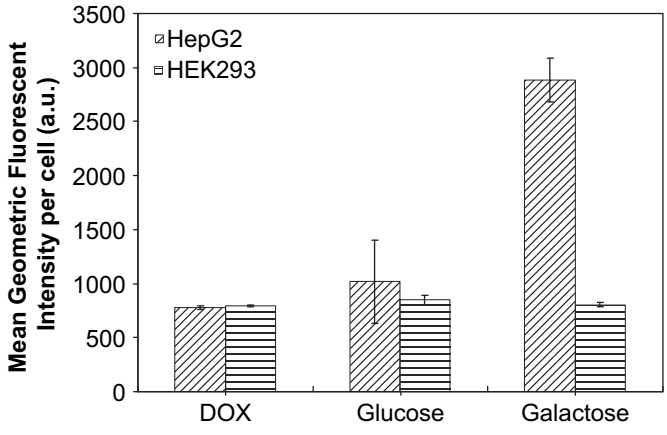


**Fig. 6.** Fluorescent intensity of HepG2 and HEK293 cells after incubated with free DOX, DOX-loaded glucose-containing micelles and DOX-loaded galactose-containing micelles for 3 h at a DOX concentration of 1 mg/L.

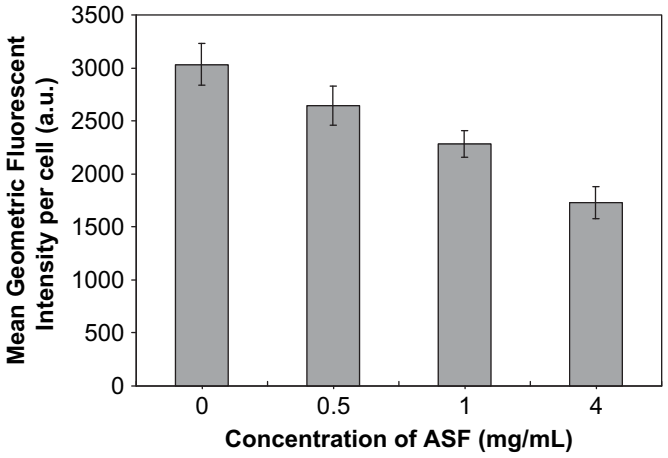


**Fig. 7.** Inhibitory effect of asialofetuin on the uptake of DOX-loaded galactose-containing micelles by HepG2 cells. HepG2 cells were incubated with asialofetuin for 1 h before DOX-loaded galactose-containing micelles were added and incubated for 3 h.

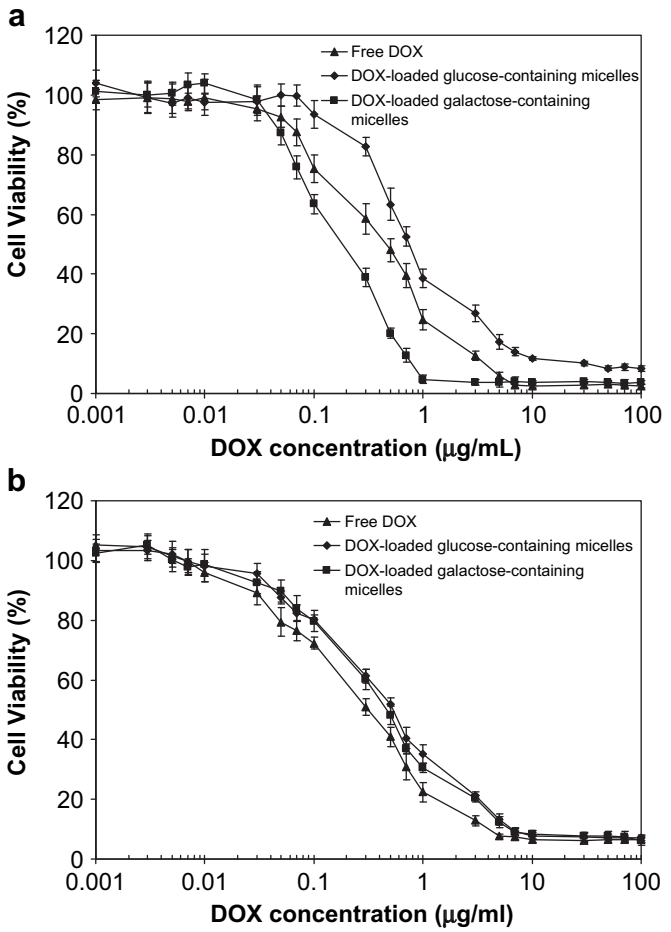


**Fig. 8.** Viability of (a) HepG2 and (b) HEK293 cells after incubated with free DOX and DOX-loaded sugar-containing micelles at various DOX concentrations.

## 4. Conclusion

We have reported the full synthesis of a family of amphiphilic sugar-bearing block copolymers by metal-free organocatalyzed ROP, and demonstrate for the first time that sugar-functionalized polycarbonate block copolymers can self-assemble into micelles in aqueous solutions, which have a mean size below 100 nm with narrow size distribution. These micelles do not show significant cytotoxicity against the two cell lines tested in this study. Therefore, they have great potential as carriers for targeted drug delivery. As an example, we demonstrate that the galactose-containing micelles can deliver DOX more efficiently into ASGP-R postive HepG2 cells than in ASGP-R negative HEK293 cells. In addition, the cytotoxicity of DOX against HepG2 cells was significantly increased when delivered using the galactose-containing micelles as compared to the free DOX formulation and the glucose-containing micelles. The cellular uptake of the galactose-containing micelles was through ASGP-R mediated endocytosis. The galactose-containing micelles can be a promising carrier to target drugs specifically to liver tissues/cells.

## Acknowledgments

This work was partially supported by both the *Région Wallonne* and *Fonds Social Européen* in the frame of *Objectif 1-Hainaut*: *Materia Nova* program. F.S. is "aspirant" by the Belgian F.N.R.S. FS and PD thank both the "Belgian Federal Governement Office Policy of Science (SSTC)" for general support in the frame of the PAI-5/03 and the "Communauté Française de Belgique" for financial support. TJPK, NW and YYY thank the financial support from Institute of Bioengineering and Nanotechnology, Agency for Science, Technology and Research, Singapore.

## Appendix

Figures with essential colour discrimination. Figs. 1 and 5 in this article may be difficult to interpret in black and white. The full colour images can be found in the on-line version, at doi:10.1016/j.biomaterials.2009.12.022.

## Appendix. Supporting data

The supplementary data associated with this article can be found in the on-line version, at doi:10.1016/j.biomaterials.2009.12.022.

## References

[1] Kataoka K, Harada A, Nagasaki Y. Block copolymers micelles for drug delivery: design, characterization and biological significance. Adv Drug Deliv Rev 2001;47:113–31.
[2] Xue C, Jog SP, Murthy P, Liu H. Synthesis of highly water-soluble fluorescent conjugated glycopoly(p-phenylene)s for lectin and escherichia coli. Biomacromolecules 2006;7:2470–4.
[3] Auzély-Velty R, Cristea M, Rinaudo M. Galactosylated *N*-vinylpyrrolidone–maleic acid copolymers: synthesis, characterization, and interaction with lectins. Biomacromolecules 2002;3:998–1005.
[4] Jelinek R, Kolusheva S. Carbohydrate biosensors. Chem Rev 2004;104:5987–6016.
[5] Yamada K, Minoda M, Miyamoto T. Controlled synthesis of amphiphilic block copolymers with pendant *N*-Acetyl-D-glucosamine residues by living cationic polymerization and their interaction with WGA lectin. Macromolecules 1999;32:3553–8.
[6] Branderhorst HM, Liskamp RMJ, Visser GM, Pieters RJ. Strong inhibition of cholera toxin binding by galactose dendrimers. Chem Commun 2007;47:5043–5.
[7] Woller EK, Cloninger MJ. The lectin-binding properties of six generations of mannose-functionalized dendrimers. Org Lett 2002;4:7–10.
[8] Wolfenden ML, Cloninger MJ. Mannose/lucose-functionalized dendrimers to investigate the predictable tunability of multivalent interactions. J Am Chem Soc 2005;127:12168–9.
[9] Woller EK, Walter ED, Morgan JR, Singel DJ, Cloninger MJ. Altering the strength of lectin binding interactions and controlling the amount of lectin clustering using mannose/hydroxyl-functionalized dendrimers. J Am Chem Soc 2003;125:8820–6.
[10] Roy R. Glycodendrimers: a new class of biopolymers. Polym News 1996;21:226–32.
[11] Roy R. Syntheses and some applications of chemically defined multivalent glycoconjugates. Curr Opin Struct Biol 1996;6:692–702.
[12] Narain R, Armes SP. Synthesis and aqueous solution properties of novel sugar methacrylate-based homopolymers and block copolymers. Biomacromolecules 2003;4:1746–58.
[13] Mortell KH, Weatherman RV, Kiessling LL. Recognition specificity of neoglycopolymers prepared by ring-opening metathesis polymerization. J Am Chem Soc 1996;118:2297–8.
[14] Muthukrishnan S, Jutz G, Andr é X, Mori H, Müller AHE. Synthesis of hyperbranched glycopolymers via self-condensing atom transfer radical copolymerization of a sugar-carrying acrylate. Macromolecules 2005;38:9–18.
[15] Muthukrishnan S, Mori H, Müller AHE. Synthesis and characterization of methacrylate-type hyperbranched glycopolymers via self-condensing atom transfer radical copolymerization. Macromolecules 2005;38:3108–19.
[16] Serizawa T, Yasunaga S, Akashi M. Synthesis and lectin recognition of polystyrene core-glycopolymer corona nanospheres. Biomacromolecules 2001;2:469–75.
[17] Serizawa T, Uchida T, Akashi M. Synthesis of polystyrene nanospheres having lactose-conjugated hydrophilic polymers on their surfaces and carbohydrate recognition by proteins. Biomater Sci Polymer Edn 1999;10:391–401.
[18] Joralemon MJ, Murthy SK, Remsen EE, Becker ML, Wooley KL. Synthesis, characterization, and bioavailability of mannosylated shell cross-linked nanoparticles. Biomacromolecules 2004;5:903–13.
[19] Nagasaki Y, Yasugi K, Yamamoto Y, Harada A, Kataoka K. Sugar-installed block copolymer micelles: their preparation and specific interaction with lectin molecules. Biomacromolecules 2001;2:1067–70.
[20] Seymour LW, Duncan R, Chytry V, Strohalm J, Ulbrich K, Kopeček J. Intraperitoneal and subcutaneous retention of a soluble polymeric drug-carrier bearing galactose. J Control Release 1991;16:255–62.

[21] Dragsten PR, Mitchell DB, Covert G, Baker T. Drug delivery using vesicles targeted to the hepatic asialoglycoprotein receptor. Biochim Biophys Acta 1987;926:270–9.
[22] Alving CR, Schneider I, Schwartz Jr GM, Steck EA. Sporozoite-induced malaria: therapeutic effects of glycolipids in liposomes. Science 1979;205:1142–3.
[23] Lin YS, Tungpradit R, Sinchaikul S, An FM, Liu DZ, Phutrakul S, et al. Targeting the delivery of glycan-based paclitaxel prodrugs to cancer cells via glucose transporters. J Med Chem 2008;51:7428–41.
[24] Wang YC, Liu XQ, Sun TM, Xiong MH, Wang J. Functionalized micelles from block copolymer of polyphosphoester and poly(ε-caprolactone) for receptor-mediated drug delivery. J Control Release 2008;128:32–40.
[25] Zhang XQ, Wang XL, Zhang PC, Liu ZL, Zhuo RX, Mao HQ, et al. Galactosylated ternary DNA/polyphosphoramidate nanoparticles mediate high gene transfection efficiency in hepatocytes. J Control Release 2005;102:749–63.
[26] Wu DQ, Lu B, Chang C, Chen CS, Wang T, Zhang YY, et al. Galactosylated fluorescent labeled micelles as a liver targeting drug carrier. Biomaterials 2009;30:1363–71.
[27] Hattori Y, Kawakami S, Lu Y, Nakamura K, Yamashita F, Hashida M. Enhanced DNA vaccine potency by mannosylated lipoplex after intraperitoneal administration. J Gene Med 2006;8:824–34.
[28] Pratt RC, Nederberg F, Waymouth RM, Hedrick JL. Tagging alcohols with cyclic carbonate: a versatile equivalent of (meth)acrylate for ring-opening polymerization. Chem Commun 2008;1:114–6.
[29] Pratt RC, Lohmeijer BGG, Long DA, Lundberg PNP, Dove AP, Li H, et al. Exploration, optimization, and application of supramolecular thiourea–amine catalysts for the synthesis of lactide (co)polymers. Macromolecules 2006;39:7863–71.
[30] Ihre H, Padilla D, Jesús OL, Fréchet JMJ. Fast and convenient divergent synthesis of aliphatic ester dendrimers by anhydride coupling. J Am Chem Soc 2001;123:5908–17.
[31] Malkoch M, Malmström E, Hult A. Rapid and efficient synthesis of aliphatic ester dendrons and dendrimers. Macromolecules 2002;35:8307–14.
[32] Rokicki G. Aliphatic cyclic carbonates and spiroorthocarbonates as monomers. Prog Polym Sci 2000;25:259–342.
[33] Hino T, Endo T. A novel synthetic approach to networked polymers without volume shrinkage on cross-linking polymerization: cationic copolymerization of a monofunctional epoxide and a spiro orthocarbonate bearing norbornene backbone. Macromolecules 2003;36:5902–4.
[34] Weilandt KD, Keul H, Höcker H. Synthesis and ring-opening polymerization of 2-acetoxymethyl-2-alkyltrimethylene carbonates and of 2-methoxycarbonyl-2-methyltrimethylene carbonate; a comparison with the polymerization of 2,2-dimethyltrimethylene carbonate. Macromol Chem Phys 1996;197:3851–68.
[35] Keul H, Bächer R, Höcker H. Anionic ring-opening polymerization of 2,2-Dimethyltrimethylene carbonate. Makromol Chem 1986;187:2579–89.
[36] Kricheldorf HR, Stricker A, Lossin M. Polymers of carbonic acid. XXVII. Macrocyclic polymerization of trimethylene carbonate. J Polym Sci A 1999;37:2179–89.
[37] Wilhelm M, Zhao CL, Wang Y, Xu R, Winnik MA, Mura JL, et al. Poly(styrene-ethylene oxide) block copolymer micelle formation in water: a fluorescence probe study. Macromolecules 1991;24:1033–40.
[38] Booth C, Attwood D. Effects of block architecture and composition on the association properties of poly(oxyalkylene) copolymers in aqueous solution. Macromol Rapid Commun 2000;21:501–27.
[39] Schwartz AL, Fridovich SE, Lodish HF. Kinetics of internalization and recycling of the asialoglycoprotein receptor in a hepatoma cell line. J Biol Chem 1982;257:4230–7.
[40] Wakebayashi D, Nishiyama N, Yamasaki Y, Itaka K, Kanayama N, Harada A, et al. Lactose-conjugated polyion complex micelles incorporating plasmid DNA as a targetable gene vector system: their preparation and gene ttansfecting efficiency against cultured HepG2 cells. J Control Release 2004;95:653–64.
[41] Maruyama K, Iwasaki F, Takizawa T, Yanagie H, Niidome T, Yamada E, et al. Novel receptor-mediated gene delivery system comprising plasmid/protamine/sugar-containing polyanion ternary complex. Biomaterials 2004;25:3267–73.